Chondroitin Sulfate-Coated DNA-Nanoplexes Enhance Transfection Efficiency by Controlling Plasmid Release from Endosomes: A New Insight into Modulating Nonviral Gene Transfection

*Hongji Yan, Oommen P. Oommen, Di Yu, Jöns Hilborn, Hong Qian, and Oommen P. Varghese**

Degradation of plasmid DNA (pDNA) in the endosome compartment and its release to the cytosol are the major hurdles for efficient gene transfection. This is generally addressed by using transfection reagents that can overcome these limitations. In this article, the first report is presented which suggests that controlling the release of pDNA from endosome is the key for achieving efficient transfection. In this study, chondroitin sulfate (CS)-coated DNA-nanoplexes are developed using a modular approach where CS is coated post-pDNA/PEI nanoplex formation. To ensure good stability of the nanoplexes, imine/enamine chemistry is exploited by reacting aldehyde-modified chondroitin sulfate (CS-CHO) with free amines of pDNA/PEI complex. This supramolecular nanocarrier system displays efficient cellular uptake, and controlled endosomal pDNA release without eliciting any cytotoxicity. On the contrary, burst release of pDNA from endosome (using chloroqine) results in significant reduction in gene expression. Unlike pDNA/PEI-based transfection, the nanoparticle design presented here shows exceptional stability and gene transfection efficiency in different cell lines such as human colorectal cancer cells (HCT116), human embryonic kidney cells (HEK293), and mouse skin-derived mesenchymal stem cells (MSCs) using luciferase protein as a reporter gene. This new insight will be valuable in designing next generation of transfection reagents.

1. Introduction

Gene-based therapies hold great promise in treating diseases that are not curable with conventional treatment modalities. This method uses different carrier systems to insert plasmid DNA (pDNA) into cells that could express a therapeutic protein of interest.[1] Currently, genes can be delivered to human patients directly or to patient derived freshly isolated cells that are transfected and subsequently transfused back to the same patient.[2] Among different gene delivery carriers developed thus far, engineered viral particles are the most successful delivery agents that have been tested in a clinical setting.[3] These vectors, however, have exhibited immunogenic and toxicological complications, thus limiting their clinical translation.[4] As a result, nonviral gene delivery systems are sort after, albeit transfection efficiency of these systems is not comparable with that of viral particles. Amongst different nonviral gene delivery carriers, polyethylenimine (PEI) and numerous PEI-based hybrid nanoparticles have been the most successful transfection reagent, which may be considered the "gold standard." However, PEI elicits inherent toxicity and expresses limited in vivo transfection efficiency. All nonviral delivery carriers known today exploit the electrostatic interaction between the anionic phosphate backbone of pDNA and cationic charge on the liposome or polymer backbone that eventually condenses the pDNA into a nanoparticle.[5] The positively charged nanoplexes facilitate cellular internalization via ionic interactions with anionic cell surface proteoglycans. However, the excessive positive charge in these nanoparticles induces unwanted cellular toxicity. Therefore, several strategies have been explored to reduce the excess positive charges on these particles by consuming the surface amines using conjugation strategies with molecules such as anionic biopolymers,[6–8] polyethylene glycol chains, antibodies,[9] and growth factors.[10] Such modifications partially compromise their complexation ability resulting in a weaker nanoplex formation,[11] and variability of particle sizes[12] that could compromise the transfection efficiency.

H. Yan, Dr. O. P. Oommen, Prof. J. Hilborn, Prof. O. P. Varghese
Department of Chemistry
Ångström Laboratory
Science for Life Laboratory
Uppsala University
S-75121 Uppsala, Sweden
E-mail: oommen.varghese@kemi.uu.se
Dr. D. Yu
Department of Immunology
Genetics and Pathology
Science for Life Laboratory
Uppsala University
S-75123 Uppsala, Sweden
Prof. H. Qian
Center for Hematology and Regenerative Medicine
Department of Medicine
Karolinska Institute
S-14186 Huddinge, Stockholm, Sweden

DOI: 10.1002/adfm.201500695

Other prerequisites required for achieving efficient transfection involve disassembly of polyplex upon internalization, release of intact pDNA from endosome, counter extra/intracellular degradation, minimal immune activation, and effective nuclear transport.[13] Among these, endolysosomal escape is identified as a key step because these organelles are rich in degrading enzymes as well as toll-like receptors (TLR 7, 8, and 9), which activate immune response after binding with DNA sequences.

To achieve endosomal escape, Behr et al. proposed the cationic polymer-mediated endosomal disruption hypothesis also known as "proton sponge effect."[14] This effect is believed to be due to the neutralization of acidic compartment, which triggers influx of Cl^- ions, resulting in swelling of endolysosomal compartments, with eventual release of pDNA. This type of pDNA escape mechanism results in rupture of these organelles, causing the burst release of the plasmid into the cytosol. Recently, new evidence suggests that fast release of plasmid may not be ideal for effective gene expression. Controlling the plasmid release rate from the endosome by simply adding noncoding DNA along with coding DNA and cationic polymer has shown to prolong DNA release, resulting in enhanced transfection efficiency.[15,16] This controlled release could be due to the endosome destabilization resulting in pore formation that leaks nanoparticles without rupture of these organelles.[17] However, no simple strategies exist, which could prolong the sustained plasmid release from the endosome compartment without using any nonfunctional excipients, available.

In this article, we present a modular strategy using aldehyde-modified chondroitin sulfate (CS-CHO) as a multifunctional agent that can covalently coat pDNA/PEI binary complex and improve gene expression. Chondroitin sulfate (CS) is a natural glycosaminoglycan present in extracellular matrix that is known to bind cell surface CD44 receptor and internalise cargo through receptor-mediated endocytosis. The CS-CHO covalently conjugated the excess secondary amines of PEI using imine/enamine chemistry and markedly improved the stability of the nanoplex as compared with the pDNA/PEI/CS complex, which was stabilized only by electrostatic interactions. This ensued higher gene transfection efficiency with reduced cellular toxicity compared with the PEI.

2. Results and Discussion

Coating of pDNA/PEI binary nanoplexes by several anionic polymers such as hyaluronic acid,[12] CS,[13] and alginic acid[18] has been reported previously. These methods either used coating of binary nanoplexes with anionic polymers exploiting the electrostatic interactions or PEI is conjugated to an anionic polymer, which was treated with pDNA to form ternary nanoplexes. The problem with the former method is that the ionic nanoplexes obtained are not stable under high salt concentration or in the presence of anionic polymers (e.g., heparin).[7a] However, the problem associated with the latter strategy is that PEI–polymer conjugation neutralizes the overall charge resulting in poor pDNA/PEI conjugation. We, therefore, envisioned developing a modular strategy to obtain stable ternary nanoplexes after pDNA/PEI binary nanoplex formation.

2.1. Preparation of CS-CHO Derivative and Its Interaction Studies with PEI

We developed CS-CHO under mild conditions following our recently published procedure.[19] This modified biopolymer can covalently bind terminal primary amines of linear PEI by Schiff-base chemistry (imine formation), whereas the predominant secondary amines would form enamine linkages (**Scheme 1**). The imine bonds are reversible and unstable in aqueous conditions; however, enamines bonds are relatively more stable under these conditions. The aldehyde modification of CS contributes to the covalent conjugation as well as electrostatic interactions between the sulfate groups of CS and free amino groups of PEI. To verify the covalent conjugation between CS-CHO and PEI, we performed ^{1}H-NMR and

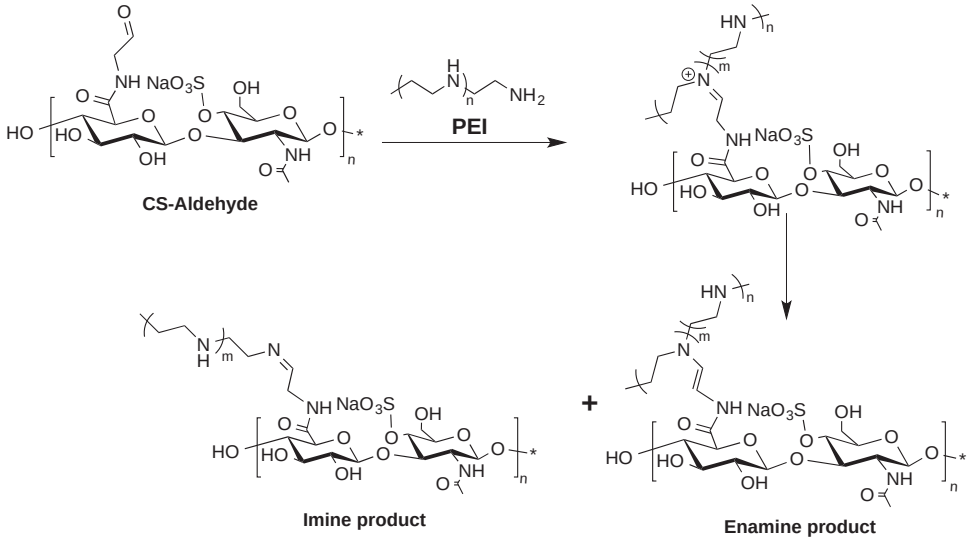

Scheme 1. Proposed mechanism indicating covalent conjugation between CS-CHO and PEI resulting in imine and enamine products.

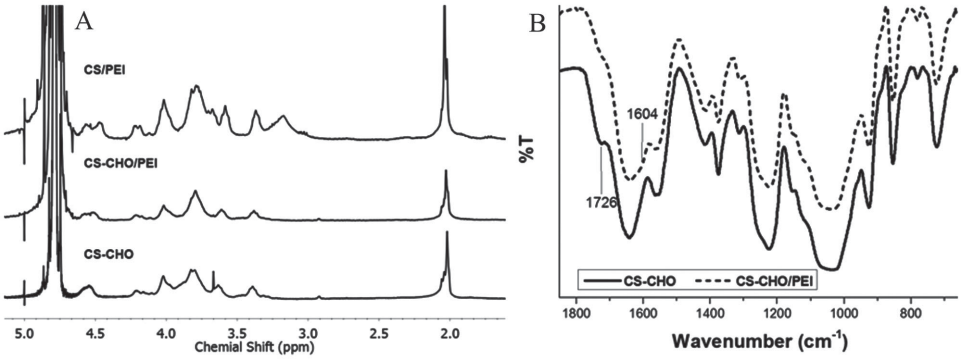

Figure 1. Characterization of CS-CHO–PEI interaction. A) ^{1}H NMR and B) ATR-FTIR analysis covalent conjugation of CS-CHO and PEI.

ATR-FTIR analysis of CS-CHO–PEI complexes and compared it with CS–PEI ionic complexes without using pDNA. In case of CS–PEI, we observed the formation of colloidal suspension upon the addition of PEI. The ^{1}H-NMR analysis showed methylene CH_2 protons of PEI at 3.1 ppm along with CS signals as anticipated (**Figure 1**). However, when CS-CHO was mixed with PEI, we observed immediate precipitation of the product at high concentrations used for ^{1}H-NMR studies. ^{1}H-NMR analysis of this sample showed only CS signals, whereas the PEI signals disappeared. This could be either due to poor solubility of the CS–PEI adduct, or due to the formation of compact core–shell assembly, which can result in disappearance of ^{1}H NMR signal of the PEI core.[20] Notably, the hemiacetal signal of hydrated aldehyde observed at 3.6 ppm also disappeared after the addition of PEI, indicating consumption of aldehyde functional group (Figure 1). ATR-FTIR analysis of the precipitate clearly demonstrated that the aldehyde signal at 1726 cm^{-1} from CS-CHO disappeared after the addition of PEI. We could also observe a new peak at 1604 cm^{-1}, which could be attributed to the enamine product (Scheme 1 and Figure 1). The reaction of secondary amine and aldehyde rendering enamine product under aqueous condition is well documented in the literature.[21]

2.2. Preparation and Characterization of Ternary Complexes

To prepare pDNA/PEI binary nanoplexes we selected the nitrogen to phosphate molar ratio of 10 (N/P = 10) as it is reported to the give the highest transfection efficiency in vitro.[22] The DLS studies of these binary nanoplexes showed an average size distribution of –60 nm and ζ-potential of +42.8 mV (**Figure 2**B). Of note, the pDNA/PEI binary complex underwent gradual aggregation and precipitated out within 30 min (data not show). To develop ternary nanoplexes, CS-CHO or CS was added to the binary nanoplexes at different weight ratios (Figure 2A). Among different weight ratios tested, nanoplexes having 5 and 25 wt% CS showed spontaneous aggregation with fluctuating ζ-potential. However, the 10 wt% CS and CS-CHO provided the most stable ternary nanoplexes, as observed by DLS analysis. The sizes of the CS and CS-CHO coated nanoplexes were 59.73 ± 2.736 and 60.18 ± 1.407 nm, respectively, and the ζ-potentials of the corresponding nanoplexes were –26.9 and –33.8 mV, respectively (Figure 2B).

To verify the stability of the nanoplexes upon storage, we performed DLS analysis after incubating the nanoparticles for 24 h at room temperature. The DLS study of pDNA/PEI binary complex could not be carried out due to its poor stability. On the contrary, pDNA/PEI/CS nanoplexes and pDNA/PEI/CS-CHO remained stable up to ≈90% and ≈98% after 24 h as compared with the freshly prepared nanoplexes (estimated by the percentage of aggregated and nonaggregated particle distribution by DLS measurement) (Figure 2B,C). To further elucidate the role of covalent conjugation for particle stability, we performed ζ-potential measurement by DLS in high salt conditions (500×10^{-3} M NaCl). We anticipated that the addition of salt would disrupt the ionic interactions, whereas the covalent interactions would remain intact. The ζ-potential remained stable in PBS buffer for 24 h; however upon addition of NaCl solution, the ζ-potential spiked indicating disruption of electrostatic association. Upon the addition of salt, the ζ-potential of pDNA/PEI/CS nanoplexes markedly increased from –26.9 to –13.8 mV, whereas the pDNA/PEI/CS-CHO nanoplexes showed a marginal increase from –25.7 to –21.6 mV (Figure 2D). This indicates the synergistic contribution of electrostatic and covalent interaction in CS-CHO/PEI association.

We also analyzed the above-mentioned particles by agarose gel electrophoresis assay, where nanoplexes having higher molecular weight fraction would show lower mobility. In this assay, free DNA is stained by SYBR Gold. As anticipated, compact pDNA/PEI nanoplexes with condensed DNA displayed poor mobility in the gel and were not stained by the dye (**Figure 3**, lane 2). The free DNA showed higher mobility, which was easily stained by the dye (Figure 3, lane 1). On the other hand, pDNA/PEI/CS nanoplexes demonstrated presence of condensed DNA as well as some free DNA that was stained by SYBR Gold (Figure 3, lane 3). This is mainly due to the fact that the addition of excess anionic polymer can disrupt the existing ionic complex between pDNA and PEI. A similar observation has been reported previously where heparin or CS was used to evaluate the stability of ionic nanoplexes.[7a] The pDNA/PEI/CS-CHO nanoplexes, on the other hand, showed robust complex formation similar to the pDNA/PEI binary complex (Figure 3, lane 4). This clearly indicates that covalent conjugation of CS on pDNA/PEI can overcome the ionic disruption caused by the electrostatic interaction of native CS.

To further analyze the topography of our nanoplexes, we performed AFM experiments. Notably, all the nanoplexes

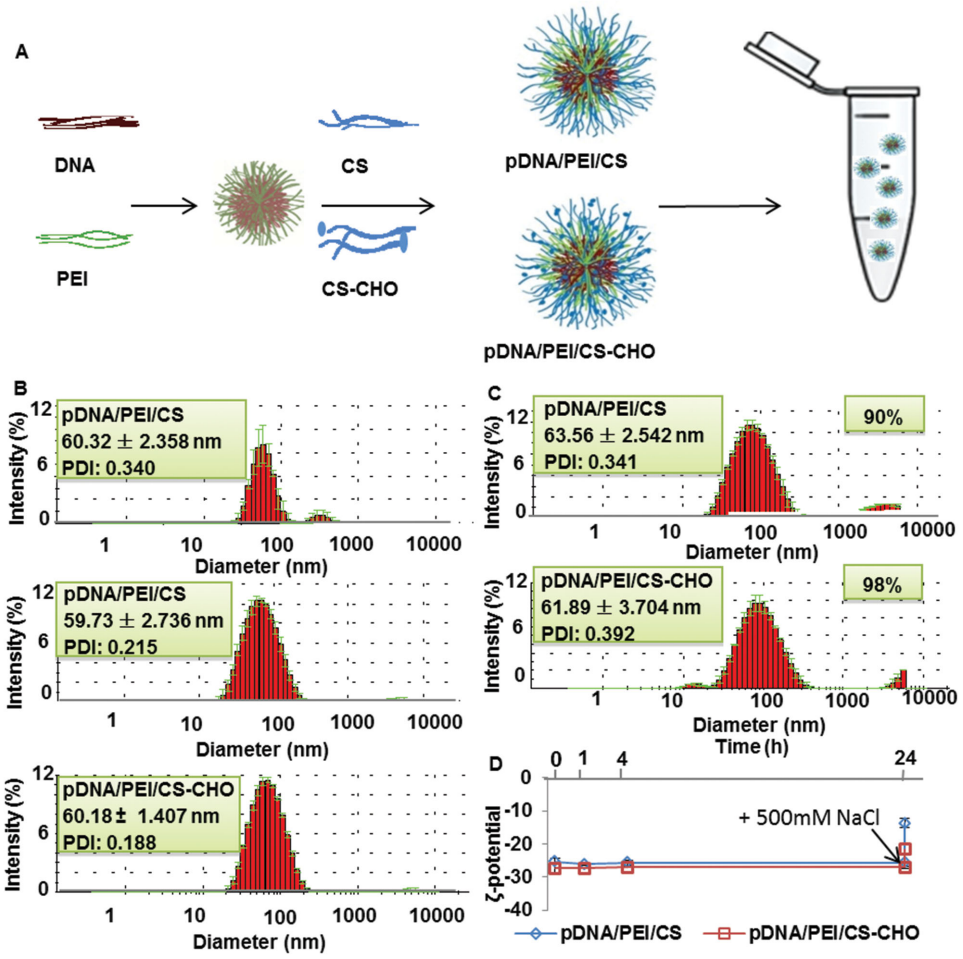

Figure 2. Ternary nanoplexes preparation strategy and particles size and ζ-potential analysis of nanoplexes by DLS. A) Schematic representation of pDNA/PEI, pDNA/PEI/CS, and pDNA/PEI/CS-CHO nanoplexes. B) Size distribution of pDNA/PEI, pDNA/PEI/CS, and pDNA/PEI/CS-CHO nanoplexes at the ratio of N/P = 10. C) Size distribution of pDNA/PEI/CS and pDNA/PEI/CS-CHO nanoplexes after 24 h incubation at room temperature. D) Kinetic studies of ζ-potential of pDNA/PEI/CS and pDNA/PEI/CS-CHO nanoplexes.

showed homogenous round morphology with the average size of 7–15 nm (**Figure 4**). The size distribution observed was markedly smaller than that was observed by DLS (60 nm). This can be attributed to the difference in hydration of polyelectrolyte coat in DLS measurement and dry analysis in AFM measurement. The size obtained by DLS study would resemble the natural hydration of the particles in cell culture system.

2.3. CD44 Expression Levels in Different Cells and the Cellular Uptake of Nanoplexes

Since efficient cellular delivery of nanoplexes with minimal toxicity is the major evaluation criteria for any gene delivery carrier, we selected human colon cancer cells (HCT116)[23] and human embryonic kidney cells (HEK 293). In addition to cell lines, we also tested mouse skin-derived primary stem cells (MSCs), as they are known to be difficult to transfect cells with high therapeutic potential. Before performing transfection experiments, we estimated the relative CD44 expression levels

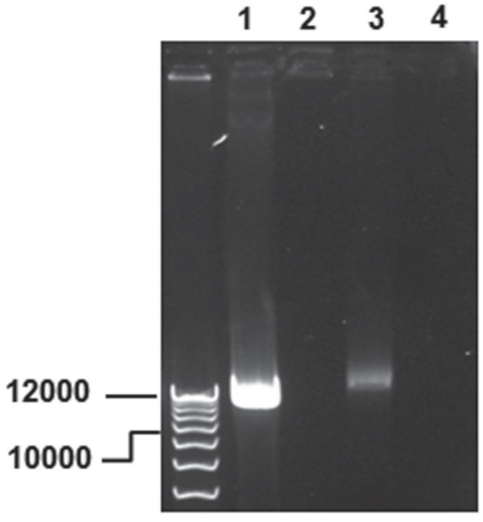

Figure 3. Agarose gel electrophoreses indicating stability of nanoplexes. Lanes 1, 2, 3, and 4 show pDNA, pDNA/PEI, pDNA/PEI/CS, and pDNA/PEI/CS-CHO, respectively, after staining with SYBR Gold.

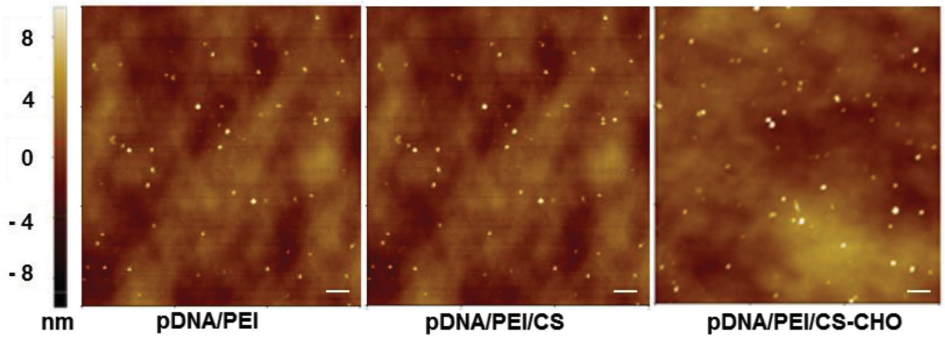

Figure 4. Microscopic images of nanoplexes. AFM images of pDNA/PEI, pDNA/PEI/CS, and pDNA/PEI/CS-CHO nanoplexes. Scale bar: 500 nm.

of the different cells. For this purpose, we performed FACS analysis using the FITC-conjugated anti-CD44 antibody. These experiments revealed differences in CD44 expression levels. HCT116 cells had a high CD44 expression level than other cell types, although HEK293 cells and the MSCs also showed a moderate-to-high expression as well.

We further evaluated whether cellular uptake of CS-coated nanoplexes was associated with CD44 cellular expression levels. For this purpose, we tested cellular uptake of Cy3-labeled binary and ternary nanoplexes using FACS after 1 h of incubation. However, for the ternary nanoplexes, HCT116 cells showed enhanced cellular uptake, suggesting a CD44-mediated endocytosis (**Figure 5**C,D, green curve). On the other hand, HEK293 cells and the MSCs also demonstrated cellular uptake of nanoplexes but to a lower extent, correlating to the CD44 expression pattern in these cells (Figure 5A,C,D, blue and red curves).

2.4. Toxicity Studies of Nanoplexes

Since cellular toxicity of gene delivery vehicle is the key aspect that limits the full potential of gene-based biomedicine, we performed cytotoxicity studies using our nanoplexes. For this purpose, we performed transfection experiments with HCT116 cells, HEK293 cells, and primary MSCs after incubation with the nanoplexes for 24 h and evaluated the viable cells by measuring the lactate dehydrogenase (LDH) levels after cell lysis. The LDH levels correlate to the early necrosis and late apoptosis event, as a result of treatment.[24] The evaluation of LDH assay revealed that unlike PEI-coated binary nanoplexes, the LDH levels of CS- and CS-CHO-coated ternary nanoplexes were similar to untreated negative control in all the three cell types tested demonstrating biocompatibility of CS- and CS-CHO-coated particles (**Figure 6**).

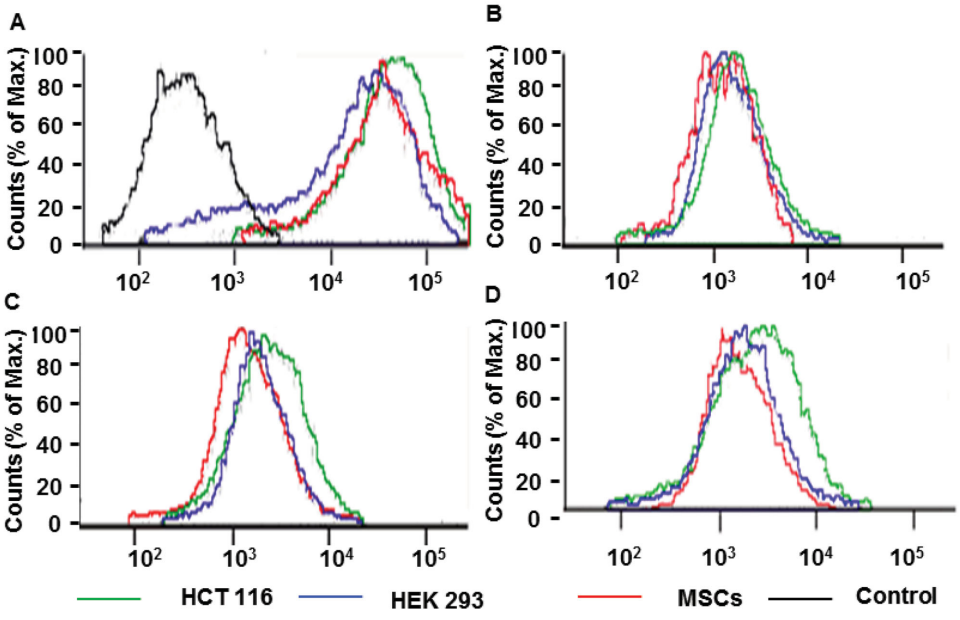

Figure 5. Determination of cell surface CD44 receptor in different cell types and its relation to cellular uptake of nanoplexes. A) Representative FACS histogram showing CD44 expression level analysis with respect to isotype control (black). Cellular uptake of Cy3-labeled nanoplexes in different cell lines, B) pDNA/PEI, C) pDNA/PEI/CS, and D) pDNA/PEI/CS-CHO, as determined by flow cytometry. Three independent experiments were carried out for each nanoplex.

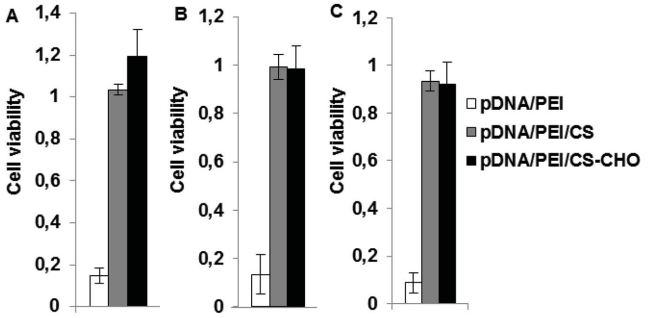

Figure 6. Cell viability of the A) HCT116, B) HEK293, and C) MSCs after treatment with different nanoplexes for 24 h of incubation.

2.5. In Vitro Gene Transfection Studies in Different Cell Types

We then evaluated if cellular uptake characteristics of different nanoplexes could be translated to efficient gene expression in vitro. For this purpose, we selected codon-optimized firefly Luc2 plasmid and performed gene transfection studies in the above-mentioned cell types. The luciferase activity was analyzed in terms of luminescence intensity in different experimental groups. Because the cellular uptake of different nanoplexes relies on interactions between cell-surface receptor and nanoplexes, we performed transfection studies by incubating nanoplexes for 1, 4, and 24 h, respectively. These experiments clearly showed that covalently coated nanoplexes, pDNA/PEI/CS-CHO, showed the highest level of luciferase activity, followed by pDNA/PEI/CS and pDNA/PEI in all the cell types tested (**Figure 7**). The high CD44 expressing HCT116 cells showed higher transfection ability at the three tested incubation times, followed by HEK293 cells and the mouse primary skin MSCs (Figure 7A–C). This clearly corroborates with the cellular uptake characteristics observed previously. We also observed that the gene expression profiles between binary and ternary nanoplexes varied with incubation time. The 24 h incubation time was found to be the most optimal for CS- and CS-CHO-coated nanoplexes, whereas the 4 h incubation time was optimum for pDNA/PEI nanoplexes. This difference could be attributed to the inherent toxicity of PEI that is evident after longer incubation time, which is completely abolished by CS coating.

2.6. Evaluation of Endosomal Escape Characteristics of Nanoplexes

Endosomal escape of nanoplexes, preventing proteolytic degradation, has been attributed to be a key feature for effective gene transfer. Cationic polymer such as PEI can favor endosomal escape by "proton sponge effect" initiating the swelling of the endosomes.[25] Recently, Symens et al. reported that prolonged release of coding pDNA from nanoplexes by diluting the pDNA with noncoding DNA could favor transfection efficiency.[15] Thus, tuning endosomal release of pDNA could have significant implication on transfection efficiency as this could prevent premature degradation of the DNA in cytosol.

We therefore investigated whether coating pDNA/PEI nanoplexes with CS could promote controlled endosomal release of the pDNA. For this purpose, we performed transfection experiment with HCT116 cells and added LysoTracker Red (at different time points), a pH sensitive dye, which accumulates in acidic compartments of the cell such as endosomes and lysosomes (Figure S1 in the Supporting Information). The accumulation of the dye in these compartments results in red fluorescence, which indirectly indicates the presence of endolysosomal compartments at a particular time point. These experiments revealed that within the first 3 h after transfection, the acidic organelles markedly increased and gradually decreased in number with time (**Figure 8**A). Comparison of intracellular acidic organelles after incubation with different nanoplexes revealed that the presence of cationic charges (e.g., pDNA/PEI nanoplexes) showed a sharp increase in acidic compartment. This could be explained by the fact that the presence of positive charges results in swelling of endolysosomal compartments due to ion flux, resulting in an increase in the volume of acidic organelles and eventual burst release of the cargo molecules. Comparison of pDNA/PEI/CS and pDNA/PEI/CS-CHO nanoplexes revealed that covalent conjugation of binary complex with an anionic polymer delayed such swelling process of the endolysosomes, which is clearly evident after 8 h. This presumably could delay the release of the cargo molecules, allowing a controlled release, which could prevent cytosolic degradation of pDNA. Controlled release of pDNA could also result in an increased availability of these molecules during mitosis, the process that increases nuclear transport of pDNA. The improvement in transfection efficiency as a result of CS coating could also be due to nuclear accumulation of CD44 receptor in

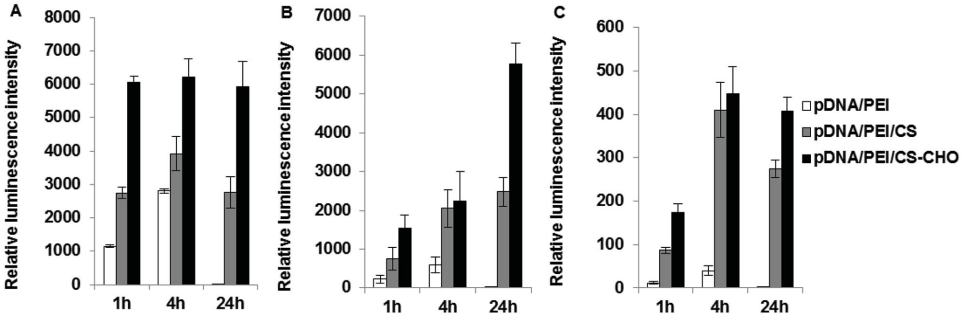

Figure 7. Comparison of gene transfection efficiency of different nanoplexes in different cell types. Luciferase activity in A) HCT116 cells, B) HEK 293 cells, and C) the MSCs transfected with different nanoplexes, namely pDNA/PEI, pDNA/PEI/CS, and pDNA/PEI/CS-CHO.

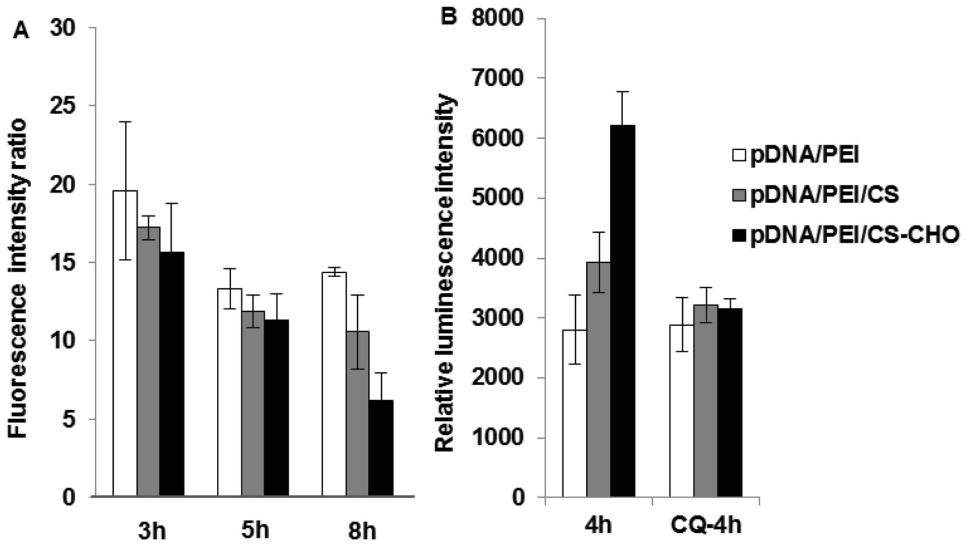

Figure 8. Endosomes disruption capacity of pDNA/PEI, pDNA/PEI/CS, and pDNA/PEI/CS-CHO nanoplexes in HCT116 cells. A) Relative fluorescence intensity of LysoTracker Red after incubation of nanoplexes for different time points. B) Luciferase activity in the presence and absence of chloroquine.

cancer cells.[26] Although the exact role of this receptor within the nuclear compartment is unclear, nuclear translocation of this cell-surface receptor occurs in a transportin-dependent manner, which could favor CD44-mediated nuclear transport of the cargo molecules.[26]

To further verify the role of endolysosomal disruption on transfection efficiency, we performed a transfection experiment in the presence of chloroquine, a known lysosomotropic agent. Chloroquine (100×10^{-6} M) was used for this experiment as we have previously shown that such a concentration does not induce any toxicity to HCT116 cells.[23] Chloroquine is known to accumulate within acidic subcellular compartments, and triggers its disruption.[27] The addition of chloroquine during the transfection experiments showed an intriguing result with different nanoplexes. When pDNA/PEI nanoplex was used, the addition of chloroquine had no impact on the transfection efficiency. This is in agreement with a previous report that supports the endosomolytic characteristic of PEI.[19] Notably, in cases of pDNA/PEI/CS and pDNA/PEI/CS-CHO nanoplexes, the transfection efficiency markedly diminished and became nearly identical to that of pDNA/PEI-based transfection experiment (Figure 8B). This demonstrates that controlled release of the nanoplexes from endolysosomal compartments is critical for improving transfection efficiency as the half-life of pDNA in the cytosol rarely exceeds 90 min.[15]

3. Conclusions

In conclusion, we present the first direct evidence suggesting that nanoplex stabilization and controlled release from endosome compartment are the key parameters for improving gene transfection efficiency using nonviral vectors. Coating of the polyplex with a tumor targeting biopolymer such as CS promotes tumor targeting ability and biocompatibility. The pDNA/PEI nanoplexes were stabilized by synergistic covalent (enamine/imine) and ionic interactions (amine/sulfate) using CS-CHO. Such a coating stabilized the pDNA/PEI binary nanoplexes and changed the net positive charge to a net negative without changing the particle size. This also eliminated PEI-induced cellular cytotoxicity. Our results provide a new insight into improving transfection efficiency by modulating the cellular release of pDNA from endosome. Such a control over pDNA release will also be significant for other lipid and cationic peptide/polymer-based delivery systems that are currently developed for clinical applications.

4. Experimental Section

Materials and Methods: All reagents and chemicals were purchased from Sigma-Aldrich, unless otherwise stated. Chondroitin sulfate-A (CS-A, 54 kDa from bovine trachea) was purchased from Sigma-Aldrich (Sweden). Dialysis membranes used for purification were purchased from Spectra Por-6 (MWCO 3500). Dulbecco's modified Eagle's medium (DMEM), antibiotics (penicillin 100 U mL^{-1} and streptomycin 100 µg mL^{-1}), and other culture reagents were obtained from Gibco BRL (Life Technologies, Sweden). DNA labeling kit was purchased from Mirus. Lactate dehydrogenase (LDH) assay kit and luciferase activity kit were obtained from Invitrogen. HCT 116 and HEK293 cells were obtained from American Type Culture Collection (ATCC-LGC Standards, Sweden). The mouse derived skin primary MSCs were provided by Prof. Hong Qian and characterization of these cells will be published elsewhere. Linear PEI of 25 kDa was used in this study. The NMR experiments were carried out on Jeol JNM-ECP Series FT NMR system at a magnetic field strength of 9.4 T, operating at 400 MHz for ^{1}H. FTIR analyses were carried out on PerkinElmer Spectrum One AT-FTIR instrument and DLS measurement was carried out in Zetasizer Nano-ZS from Malvern.

Plasmid Preparation: pDNA sequence that encodes copepod green fluorescent protein (copGFP) and codon-optimized firefly luciferase (Luc2) was previously developed[28] based on pSh(CMV). The transgene expression is under the control of cytomegalovirus immediate early constitutive promoter and separated by a self-cleaving peptide derived from Thosea asigna virus.

Synthesis and Characterization of CS-CHO: Synthesis of CS-CHO was performed according to our recently reported two-step procedure.[19] Briefly, CS (500 mg, 1 mmol of disaccharide repeating

units) was dissolved in 100 mL of deionized water. To this solution, *N*-hydroxybenzotriazole (153 mg, 1 mmol) and 3-amino-1,2-propanediol (91 mg, 1 mmol) were added, and it was stirred until it was completely dissolved (approximately for 30 min). The pH of the resultant solution was adjusted to 6 by 1 M HCl. The coupling reagent, 1-ethyl-3-(3-dimethylaminopropyl)carbodiimide (57.5 mg, 0.3 mmol), was added and stirred overnight. The reaction mixture was purified by dialysis (Spectra Por-3, MWCO 3500) against dilute HCl (pH = 3.5) containing 0.1 M NaCl in (2 × 2 L) for 48 h. This was followed by dialysis against deionized water (2 L) for 24 h and was lyophilized to obtain 450 mg of the product. 3-Amino-1,2-propanediol-conjugated product (250 mg, 0.5 mmol of disaccharide repeating units) was dissolved in 45 mL of deionized water and treated with 107 mg of predissolved $NaIO_4$ (0.5 mmol dissolved in 0.5 mL water). After 10 min, reaction was quenched using fivefold excess of ethylene glycol (0.16 mL, 2.5 mmol) and the mixture was stirred for additional 1 h. The reaction product was dialyzed against deionized water (2 L) for 48 h (Spectra Por-3, MWCO 3500) and lyophilized to obtain 240 mg of the desired product. The lyophilized product was characterized by ^{1}H-NMR analysis and attenuated total reflectance Fourier transform infrared spectroscopy (ATR-FTIR), as described previously,29 and the degree of aldehyde modification was found to be 10%.

Characterization of CS–PEI and CS-CHO–PEI Interactions: CS or CS-CHO (16 mg mL^{-1}) was dissolved in deuterated water. To this solution, PEI (3 mg mL^{-1} in deuterated PBS) was added, and the pH was adjusted to 7.1 before recording the ^{1}H-NMR spectra. When CS-CHO was mixed with PEI, we observed precipitate, which was then isolated by centrifugation and dried. This material was subjected to ATR-FTIR analysis and compared with CS-CHO.

Preparation and Characterization of Binary and Ternary Nanoplexes: Linear PEI and pDNA was mixed in DNase free water such that the N/P = 10. The product obtained was further incubated at room temperature for 10 min, and the particle stability was evaluated using dynamic light scattering (DLS) measurements. These complexes were termed pDNA/PEI binary nanoplexes. These nanoplexes were subsequently coated with native CS or CS-CHO. To prepare the ternary nanoplexes, different weight ratios of CS and CS-CHO (i.e., 5, 10, and 25) were tested, with respect to pDNA, and incubated for 45 min to obtain pDNA/PEI/CS and pDNA/PEI/CS-CHO nanoplexes, respectively. For a typical experiment with 10 wt% of CS or CS-CHO, we added 2 µg of polysaccharide to pDNA/PEI nanoplexes containing 200 ng of pDNA and 265 ng of PEI. The nanoparticle sizes and their ζ-potentials were evaluated using DLS instrument (Malven, Zetasizer Nano ZS). Atomic force microscopy (AFM; Nanosurf Mobile S system) was used to characterize the topography of nanoplexes using noncontact mode. To prepare the samples for AFM, the nanoplexes were prepared as mentioned above, and these suspensions were dropped onto a silicon wafer and distributed by nitrogen gas. The air-dried samples were placed in an AFM at noncontact mode.

Electrophoretic Gel Retardation Assay: The pDNA/PEI, pDNA/PEI/CS, and pDNA/PEI/CS-CHO nanoplex formation was visualized by measuring electrophoretic gel shift assay using 0.7% agarose gel. Briefly, pDNA/PEI nanoplexes (N/P = 10) were freshly prepared using 400 ng of pDNA (as mentioned above) and 10 wt% CS-CHO or CS solutions in water. These nanoplexes were subsequently loaded into each well and the same amount of pDNA was used as control. The gel was run for 2 h at 100 mV in TBE buffer (0.22 M Tris, 180×10^{-3}M Borate, 5×10^{-3} M EDTA, pH 8.3). The gel was stained using SYBR Gold nucleic acid gel stain for 40 min at room temperature following manufacturer's protocol and visualized under UV light.

CD44 Expression Level Analysis: FITC-conjugated anti-CD44 antibody (Sigma) was used to measure cell-surface CD44 expression levels on HCT116 and HEK293 cells and the skin MSCs. Briefly, cells were detached using enzyme-free cell dissociation buffer (Life Technologies) and washed with PBS buffer. 20 000 cells were collected and resuspended in PBS buffer (500 µL) containing 0.5 µg of FITC-conjugated anti-CD44 antibody. The cell suspension was incubated at 4 °C for additional 30 min. Thereafter, cells were washed three times with PBS and analyzed using fluorescence activated cell sorting (FACS). FITC-conjugated IgG 2 antibody was used as isotype control to evaluate the unspecific binding.

Estimation of Cellular Uptake of Binary and Ternary Nanoplexes: pDNA was labeled with Cy3 using label IT kit, according to manufacturer's protocol. Briefly, DNA labeling reaction samples were prepared by mixing 35 µL of molecular biology-grade H_2O, 5 µL of 10 X labeling buffer A, 5 µL of Label IT reagent, and 5 µL of 1 mg mL^{-1} pDNA, and incubated at 37 °C for 1 h. The labeled pDNA was purified on G50 Microspin Purification Column. pDNA/PEI binary nanoplexes and pDNA/PEI/CS and pDNA/PEI/CS-CHO ternary nanoplexes were prepared as mentioned earlier. To perform cellular uptake efficiency study, 30 000 cells were seeded into 12-well plates and cultured with DMEM containing 10% foetal bovine serum (FBS) and 1% antibiotics. After 24 h, transfection medium containing nanoplexes were added and incubated for 1 h. Cells were washed three times with PBS and then detached and resuspended in FACS buffer. Quantification of cellular uptake of fluorescently labeled nanoplexes was performed by FACS analysis.

Cellular Toxicity Study: The cellular toxicity studies of different nanoplexes were determined using LDH cytotoxic assay using HCT116, HEK293 cells and primary MSCs. Briefly, cells were seeded into 96-well plates at a seeding density of 3000 cells/well and cultured as mentioned above. After 24 h, the cell culture medium was replaced with transfection medium containing pDNA/PEI nanoplexes, pDNA/PEI/CS, or pDNA/PEI/CS-CHO nanoplexes, and incubated for 24 h. Thereafter, LDH levels in each well were determined according to the LDH assay kit. Briefly, cells lysates were first obtained by repeated freeze and thaw cycle (two times). Cell lysates (100 µL) were then treated with same volume of LDH lysis solution. The mixture was incubated for 20 min at 37 °C and the absorbance level was measured at 490 nm using the Labsystems Multiskan MS plate reader. The untreated cells were used as negative controls. Cell viability was quantified by normalizing the LDH levels of different groups with negative control.

In Vitro Gene Transfection Assay: HCT116 and HEK293 cells and the MSCs were cultured in complete medium (DMEM/nutrient mixture F-12 Ham's medium, supplemented with 10% FBS) at 37 °C and 5% CO_2. For performing transfection experiments, 3000 cells/well were seeded in 96-well plates and cultured, as mentioned above, and incubated for 24 h at 37 °C under humidified atmosphere. Thereafter, the cell culture medium was replaced with fresh serum-free medium containing different nanoplex formulations such that each well contained 200 ng of Luc2-expressing pDNA and incubated at 37 °C for 1, 4, or 24 h, after which the medium was replenished with fresh complete medium and incubated for total 48 h. To quantify the level of Luc2 expression, One-Glo luciferase assay kit (Promega) was used, following the manufacturer's instructions. Briefly, after 48 h of incubation, 100 µL of luciferase substrate was added to each well and incubated for 30 min at room temperature. Thereafter, the luminescence in each well was measured using Labsystems Multiskan MS plate reader (Labsystems). The luminescence intensity was normalized with cell-alone control.

Determination of Controlled Release of pDNA from Endosome: To determine endosomal disruption capacity of different nanoplex formulation, endosomal disruption assay was performed using LysoTracker Red DND-99 kit (Life Technologies), following manufacturer's instruction. Briefly, HCT116 cells were seeded at a density of 3000 cells/well in 96-well plates and incubated in DMEM containing 10% FBS, 100 U L^{-1} penicillin and 100 µg L^{-1} streptomycin). Thereafter, the cell culture medium was replaced with fresh serum-free medium containing different nanoplex formulations such that each well contained 200 ng of pDNA and incubated at 37 °C for 2 h. The cell culture medium was replaced with fresh complete medium and incubated for 1, 3, and 6 h, respectively. Thereafter, the culture medium was changed with probe-containing medium and incubated for additional 1 h. Cells were washed two times with PBS to remove excess of chromophore, and 100 µL of fresh PBS was added for fluorescence measurement (excitation/emission: 577/590 nm) using the Labsystems Multiskan MS plate reader (Labsystems). To determine the endosomal escape property of nanoplexes, endosomal disruption experiment was performed in the presence of chloroquine, the endolysosomotropic agent. Briefly, the

gene transfection experiment was performed using HCT116 cells as mentioned above, with the exception that 100×10^{-6} M of neutralized chloroquine in PBS was added to cells along with nanoplexes. The medium was replaced with fresh complete medium (without chloroquine) after 1 h and incubated for 48 h at 37 °C under humidified atmosphere, as mentioned above. The Luciferase expression levels were measured as described earlier.

Statistical Analysis: Dunnett's pairwise multiple comparison *t* test was used to analyze statistical significance among groups.

Supporting Information

Supporting Information is available from the Wiley Online Library or from the author.

Acknowledgements

The present work was supported by Swedish Strategic Research grant "StemTherapy" and EU Framework Program-7 project "Biodesign." The authors also acknowledge China Scholarship Council (CSC) for supporting HY. We appreciate Ms. Shujiang Wang for providing CS-CHO derivative and Ms. Deepanjali Gurav for helping us with DLS measurements.

Received: February 18, 2015
Revised: April 17, 2015
Published online: May 18, 2015

[1] a) B. L. Alexander, R. R. Ali, E. W. F. W. Alton, J. W. Bainbridge, S. Braun, S. H. Cheng, T. R. Flotte, H. B. Gaspar, M. Grez, U. Griesenbach, M. G. Kaplitt, M. G. Ott, R. Seger, M. Simons, A. J. Thrasher, A. Z. Thrasher, S. Y. Herttuala, *Gene Ther.* **2007**, *14*, 1754; b) E. Alton, S. Ferrari, U. Griesenbach, *Gene Ther.* **2007**, *14*, 1555.

[2] D. Edinger, E. Wagner, *WIREs Nanomed. Nanobiotechnol.* **2011**, *3*, 33.

[3] a) M. A. Bartel, J. R. Weinstein, D. V. Schaffer, *Gene Ther.* **2012**, *19*, 694; b) M. P. Limberis, *Acta. Biochim. Biophys. Sin.* **2012**, *44*, 632.

[4] a) R. E. Donahue, S. W. Kessler, D. Bodine, K. McDonagh, C. Dunbar, S. Goodman, B. Agricola, E. Byrne, M. Raffeld, R. Moen, J. Bacher, K. M. Zsebo, A. W. Nienhuis, *J. Exp. Med.* **1992**, *176*, 1125; b) J. Y. Sun, V. Anand-Jawa, S. Chatterjee, K. K. Wong, *Gene Ther.* **2003**, *10*, 964; c) E. Marshall, *Science* **1999**, *286*, 2244.

[5] M. D. Brown, A. G. Schatzlein, I. F. Uchegbu, *Int. J. Pharmaceut.* **2001**, *229*, 1.

[6] a) M. Hornof, M. de la Fuente, M. Hallikainen, R. H. Tammi, A. Urtti, *J. Gene Med.* **2008**, *10*, 70; b) Y. Y. He, G. Cheng, L. Xie, Y. Nie, B. He, Z. W. Gu, *Biomaterials* **2013**, *34*, 1235.

[7] a) P. S. Xu, G. K. Quick, Y. Yeo, *Biomaterials* **2009**, *30*, 5834; b) O. P. Varghese, M. Kisiel, E. Martínez-Sanz, D. A. Ossipov, J. Hilborn, *Macromol. Rapid Commun*. **2010**, *31*, 1175

[8] Y. L. Lo, K. H. Sung, C. C. Chiu, L. F. Wang, *Mol. Pharmaceut.* **2013**, *10*, 664.

[9] T. Ferkol, J. C. Perales, E. Eckman, C. S. Kaetzel, R. W. Hanson, P. B. Davis, *J. Clin. Invest.* **1995**, *95*, 493.

[10] a) B. A. Sosnowski, A. M. Gonzalez, L. A. Chandler, Y. J. Buechler, G. F. Pierce, A. Baird, *J. Biol. Chem.* **1996**, *271*, 33647; b) B. Xu, S. Wiehle, J. A. Roth, R. J. Cristiano, *Gene Ther.* **1998**, *5*, 1235; c) J. Kloeckner, S. Boeckle, D. Persson, W. Roedl, M. Ogris, K. Berg, E. Wagner, *J. Controlled Release* **2006**, *116*, 115.

[11] a) O. Veiseh, F. M. Kievit, J. W. Gunn, B. D. Ratner, M. Q. Zhang, *Biomaterials* **2009**, *30*, 649; b) H. Lee, J. H. Jeong, T. G. Park, *J. Controlled Release* **2001**, *76*, 183.

[12] T. Ito, N. Iida-Tanaka, T. Niidome, T. Kawano, K. Kubo, K. Yoshikawa, T. Sato, Z. H. Yang, Y. Koyama, *J. Controlled Release* **2006**, *112*, 382.

[13] a) D. M. Lipinski, M. Thake, R. E. MacLaren, *Prog. Retin. Eye. Res.* **2013**, *32*, 22; b) C. W. Pouton, L. W. Seymour, *Adv. Drug Delivery Rev.* **2001**, *46*, 187.

[14] R. Kircheis, A. Kichler, G. Wallner, M. Kursa, M. Ogris, T. Felzmann, M. Buchberger, E. Wagner, *Gene Ther.* **1997**, *4*, 409.

[15] N. Symens, J. Rejman, B. Lucas, J. Demeester, S. C. De Smedt, K. Remaut, *Mol. Pharmaceut.* **2013**, *10*, 1070.

[16] a) Y. Rajendra, D. Kiseljak, S. Manoli, L. Baldi, D. L. Hacker, F. M. Wurm, *Biotechnol. Bioeng.* **2012**, *109*, 2271; b) E. V. B. van Gaal, R. S. Oosting, W. E. Hennink, D. J. A. Crommelin, E. Mastrobattista, *Int. J. Pharmaceut.* **2010**, *390*, 76.

[17] T. F. Martens, K. Remaut, J. Demeester, S. C. De Smedt, K. Braeckmans, *Nano Today*, **2014**, *9*, 344.

[18] S. Patnaik, A. Aggarwal, S. Nimesh, A. Goel, M. Ganguli, N. Saini, Y. Singh, K. C. Gupta, *J. Controlled Release* **2006**, *114*, 398.

[19] S. Wang, O. P. Oommen, H. Yan, O. P. Varghese, *Biomacromolecules* **2013**, *14*, 2427.

[20] V. Butun, S. P. Armes, N. C. Billingham, Z. Tuzar, A. Rankin, J. Eastoe, R. K. Heenan, *Macromolecules* **2001**, *34*, 1503.

[21] a) G. Belanger, M. Dore, F. Menard, V. Darsigny, *J. Org. Chem.* **2006**, *71*, 7481; b) A. P. Brogan, T. J. Dickerson, K. D. Janda, *Angew. Chem. Int. Ed.* **2006**, *45*, 8100.

[22] Y. A. Yue, F. Jin, R. Deng, J. G. Cai, Y. C. Chen, M. C. M. Lin, H. F. Kung, C. Wu, *J. Controlled Release* **2011**, *155*, 67.

[23] O. P. Oommen, J. Garousi, M. Sloff, O. P. Varghese, *Macromol. Biosci.* **2014**, *14*, 327.

[24] K. Abe, N. Matsuki, *Neurosci. Res.* **2000**, *38*, 325.

[25] R. Kircheis, A. Kichler, G. Wallner, M. Kursa, M. Ogris, T. Felzmann, M. Buchberger, E. Wagner, *Gene Ther.* **1997**, *4*, 409.

[26] M. Janiszewska, C. De Vito, M. A. Le Bitoux, C. Fusco, I. Stamenkovic, *J. Biol. Chem.* **2010**, *285*, 30548.

[27] S. D. B. Goldman, R. S. Funk, R. A. Rajewski, J. P. Krise, *Bioanalysis* **2009**, *1*, 1445.

[28] a) C. Jin, D. Yu, M. Cancer, B. Nilsson, J. Leja, M. Essand, *Hum. Gene. Ther.* **2013**, *24*, 766; b) D. Yu, C. Jin, M. Ramachandran, J. Xu, B. Nilsson, O. Korsgren, K. Le Blanc, L. Uhrbom, K. Forsberg-Nilsson, B. Westermark, R. Adamson, N. Maitland, X. L. Fan, M. Essand, *PLoS One* **2013**, *8*, e54952.

[29] O. P. Oommen, S. J. Wang, M. Kisiel, M. Sloff, J. Hilborn, O. P. Varghese, *Adv. Funct. Mater.* **2013**, *23*, 1273.